



INDIRECT COSTS OF FLOODS: A CASE STUDY OF HIGHWAYS ROAD USERS

Manuel Contreras-Jara^{1,2}, Tomás Echaveguren^{2,3}, Eduardo Allen^{3,4}, Alondra Chamorro^{1,2}, José Vargas-Baecheler³

- 5 Department of Construction, School of Engineering, Pontificia Universidad Católica de Chile, Santiago, postal code 7820436, Chile
 - ²Center for Integrated Disaster Risk Management (CIGIDEN), Santiago, postal code 7820436, Chile
 - ³Department of Civil Engineering, Faculty of Engineering, Universidad de Concepción, Concepción, postal code 4070386, Chile
- 4Department of Civil and Environmental Engineering, Faculty of Engineering, The University of Auckland, Auckland, postal code 1142, New Zealand

Correspondence to: Tomás Echaveguren (techaveg@udec.cl)

Abstract. Hydrometeorological events have a significant impact on road infrastructure and traffic flow. Floods can lead to the collapse or weakening of bridges, compromise river protection, and inundate riverine roads, thereby restricting or halting the traffic. These events incur additional user costs owing to the increased travel times resulting from the rerouting and reduced speeds on the affected roads. The economic impact of such natural events on road networks is typically quantified in terms of the infrastructure recovery costs. However, the expected road user cost (EUC) associated with driving on damaged roads is often neglected. This study aimed to estimate the flood risk to road networks by integrating a hydrological-hydraulic model with road and bridge vulnerability assessments and traffic assignment models to calculate the EUC. The procedure was applied to the "Aconcagua Bajo" Watershed in central Chile, considering floods with return periods ranging from 2 to 100 years, the vulnerability of bridges to scour, road waterlogging, travel times, and fuel consumption costs incurred by the road users.

1 Introduction

Hydrometeorological events (HME) originate from atmospheric and meteorological events that result in storms, droughts, heat waves, and floods that modify territory over time and affect the subsistence of people and infrastructure (Sahani et al., 2019). Floods are caused by rainfall, which increases river discharge, submerges lowland areas, and generates surface runoff that affects the built environment. Floods recurrently affect road networks and their infrastructure, causing the total or partial destruction of road segments and bridges, and consequently reducing the physical and operational road network performance during and after the event. Floods can cause bridges to collapse or weaken river protection. In some areas, the riverine roads may be flooded. Furthermore, flood-scour bridge foundations affect their structural integrity and prevent vehicular traffic (Klinga and Alipour, 2015; Hung and Yau, 2017). Furthermore, road waterlogging reduces traffic speed or prevents passage depending on the water height over the road (Pregnolato et al., 2017b; Contreras-Jara et al., 2018). In these cases, the impact on road network performance related to travel time increases because of reduced speed and traffic rerouting. The indirect





impacts of non-travel decisions can also reduce the traffic level on the network and induce an alternative cost per non-travel decision. Both impacts involve road users and, depending on the level of damage to the highway network, can be extended during the planning and delivery of repairs for damaged infrastructure.

The impact of floods on road network users depends on the magnitude of the HME, infrastructure vulnerability and exposure, and traffic distribution over the affected road network, making it important to estimate the flood risk on roads and bridges. Risk is commonly defined as the probability and severity of adverse consequences given the uncertainty (or probability) of hazardous events and their consequences (Aven, 2011). Therefore, risk analysis in road networks typically focuses on calculating economic losses in terms of the recovery costs of physical infrastructure. By contrast, economic loss estimation does not always consider road asset fragility or costs incurred by road users. This aspect has drawn interest in risk assessment literature in recent years (Lam et al. 2016, 2018a, 2018b, 2018c, 2020; Hackl et al. 2018; Zhang and Alipour, 2019 and 2020; Wang et al. 2020).

Flood risk is the probability of damage to infrastructure over a certain period in interaction with its physical vulnerability and exposure and associated economic losses (Merz et al., 2009; Tasakiris, 2014). This is expressed in terms of the expected annual damage caused by floods during the return period (Penning-Rowsell and Green, 2000).

Flood risk modeling of road networks under this approach includes four general steps: (1) hydrological and hydraulic modeling, (2) road asset vulnerability, (3) traffic assignment modeling under normal and damaged conditions, and (4) economic loss estimation. Wisetjindawat et al. (2017) identified the following hydrological modeling approaches: direct flow measurements, remote rainfall and flood perception, rainfall-runoff modeling, and post-event measurements. Arseni et al. (2020) used flow station data for hydrological modeling, which is appropriate if there are sufficient fluviometric stations and data per station to model watersheds or sub-watersheds. Wang et al. (2020) used non-global climate models to model the surface runoff. Vicendon et al. (2016) used hydrological balance-based models to predict flood flow. Hydraulic modeling procedures do not differ significantly and generally use digital elevation models combined with hydrodynamic, one-dimensional (1D), two-dimensional (2D), and ad hoc models. Teng et al. (2017) provided a detailed description of the available hydraulic models. Vulnerability represents the susceptibility of the receiver bodies to damage caused by natural or anthropogenic events (Menoni et al., 2012). Physical vulnerability represents the damage susceptibility of physical assets such as roads, bridges, and cut slopes, which are commonly induced by natural events (Berdica, 2002). This susceptibility is represented by fragility or damage probability models, which estimate the probability of reaching a particular damage state. Each asset has a unique fragility curve for a specific event (Hackl et al., 2018). Traffic assignment modeling determines the travel time and operating speed under normal and damaged road network conditions. Consequently, user costs can be estimated in terms of travel time and additional fuel consumption costs due to rerouting. The Beckmann et al. (1955) model and its updates are frequently used to estimate travel time in road networks in combination with traffic assignment models, assuming no congestion and origin-destination matrices (Hackl et al., 2018). Zhang and Alipour (2019, 2020) used this approach for traffic modeling in flood risk assessments.

Generally, flood risk is estimated in terms of the return period without considering the direct or indirect costs to people and their economic activities. Flood effects can be estimated economically; for instance, agricultural and housing losses or the





costs of evacuation and attending to the people affected are commonly considered direct costs. In contrast, the effect of floods on highway infrastructure and the cost transferred to road users in terms of travel time increase and additional fuel consumption are not included in the economic loss models. Consequently, the total economic losses for different flood scenarios regarding the return periods were underestimated.

In this study, we estimated the road user costs for networks affected by floods. The procedure integrates the vulnerability models of bridges and roads, a locally calibrated rainfall-runoff model for uncontrolled watersheds, and a traffic assignment model. The procedure was applied to a road network 1823 km in length, located in the "Aconcagua Bajo" watershed in central Chile. The flood scenarios included return periods of two and 100 years. The discharge was modeled using a rainfall-runoff model calibrated for Chile by Verni and King (1977) (Sections 5.1 and 5.2). Flood maps were obtained by using the HEC-RAS 2D model for each return period. Road network exposure was determined by overlapping flood and road network maps to identify flooded road network sectors and bridges affected by scour (Sections 6.1 and 6.2). The vulnerability of waterlogged roads was estimated using the traffic interruption model developed by Contreras-Jara et al. (2018) (Section 7.1). Bridge vulnerability was estimated using the scour probability model developed by Chamorro et al. (2020) (Section 7.2). Traffic assignment was obtained by combining the travel time model of Nie et al. (2004) with the numerical solution of a static traffic assignment problem implemented by Kumar (2019) (Sections 7.3 and 7.4) under normal and damaged network conditions. Travel time and fuel consumption costs were estimated and combined with the estimated road and bridge vulnerabilities to obtain a proxy for the impact of floods on the road network in the "Aconcagua Bajo" watershed in terms of road user cost losses (Sections 7.5 and 7.6). The results, discussion, and conclusions are presented in Sections 7.7 and 8, respectively.

2 Flood risk in highways networks

2.1 The flood risk concept

Risk is defined as the probability of the occurrence of an event multiplied by the consequences of the event on the system (Aven, 2011; Kron, 2005). Consequences comprise three factors (Gouldby and Samuels, 2005): exposure, vulnerability, and risk-receptor consequences.

According to Hall et al. (2006), risk can be calculated using Eq. (1), where g(x) is the limit state function of a system with "x" characteristics, and I(.) is an indicator whose value is one if $g(x) \le 0$; otherwise, it is zero. This implies that the system fails when g(x) is less than zero. The term f(x) is the probability density function that describes how the "x" system characteristics vary, and D(x) is the damage function of the system.

$$Risk = \int I(g(x) \le 0)f(x)D(x)dx \tag{1}$$

A similar definition of risk was provided by Merz et al. (2009), who applied the expected annual damage (EAD) introduced by Penning-Rowsell and Green (2000) caused by floods. Flood risk is expressed by Eq. (2), where the decision variable is the



110

115

120



water level (h), f(h) is the probability density function of the flood water level, and D(h) is the flood damage. There is a minimum water level value (h_d) at which the damage increases as the water level rises.

$$Risk = \int_{h_d}^{\infty} f(h)D(h)dh$$
 (2)

Because flood scenarios are infrequent, Eq. (2) is expressed in discrete terms, as shown in Eq. (3) for the "m" probability increments and "j" intervals (Merz et al., 2009; Lugeri et al., 2010; Scorzini and Leopardi, 2017).

$$Risk = \sum_{j=1}^{m} \Delta P_{j} D_{j} ; D_{j} = \frac{1}{2} [D(h_{j}) + D(h_{j+1})] ; \Delta P_{j} = P(h_{j}) - PD(h_{j+1})$$
(3)

where D_j is the average damage and ΔP_j is the increment in the exceedance probability. Scorzini and Leopardi (2017), Arrighi et al. (2018), and Ziya and Safaie (2023) applied Eq. (3) Flood damage (D_i) is estimated using three return periods (T_i) to obtain Eq. (4).

$$Risk = \frac{1}{T_1} \times D_1 + \left[\frac{1}{T_2} - \frac{1}{T_1}\right] \times \frac{D_1 + D_2}{2} + \left[\frac{1}{T_3} - \frac{1}{T_2}\right] \times \frac{D_2 + D_3}{2}$$
(4)

2.2 Flood risk in highway networks modeling

Bridges and road segments near rivers are exposed to flooding. Bridge foundations are affected by scouring, which weakens their structural resistance and limits heavy hauling vehicles and transit traffic. Under extreme conditions, a bridge can be closed, and consequently, traffic is diverted to other roads in the network. Flooded roads decrease vehicle driving speed and eventually interrupt traffic, forcing rerouting on the nearby roads. Owing to traffic rerouting, the total travel time and fuel consumption increase, resulting in higher road user costs. Engineers face challenges in estimating traffic reassignment, and road user costs increase as a proxy for the expected annual damage (EAD) in flooded highway networks.

Table 1 summarizes the state-of-the-art of highway flood risk modeling. The flood risk has been studied using topological, phenomenological, and hybrid approaches. The topological approach identifies link interactions in the road network and the connectivity loss of a closed set of links and nodes (Lertworawanich, 2012; Nelson et al., 2019). This phenomenological approach uses climatic or hydrological-hydraulic models to identify flooded road network links and those that are potentially disabled (Pedrozo-Acuña et al., 2017; Versini et al., 2010). The hybrid approach integrates topological and phenomenological approaches, as well as traffic assignment modeling, to determine the user costs induced by floods in highway networks (Pregnolato et al., 2017b; Hakl et al., 2018; Wang et al., 2020; van Ginkel et al., 2021; Zhang and Alipur, 2020, 2022; Moghtadernejad et al., 2022; Shahdani et al., 2022). The hazard is thus modeled using common hydrological and hydraulic models and their variations, using return periods ranging between 2 and 50 years, and exceptionally up to 10.000 years.





Table 1: State of the art of flood risk models of highway networks

Author	Risk M	odel		Hazard			Vulnerability Mode	ls
	Туре	Specification	Type	Flood model	Return Periods (T, years)	Costs	Traffic assignment	Vulnerability
Lertworawanich (2012)	Topological	Travel time increase	Flood	Not used	Not used	Travel time w/BPR	Particle swarm optimization	Not estimated
Nelson et al. (2019)	Topological	Risk matrix in terms of hazard and betweenness centrality	Floods Landslides Mudslide	NOOA climate model	100	Not used	Not used	Not used
Versini et al. (2010)	Phenomenological	Exposure	Floods	Plan d'Intervention aux Crises Hydrologiques inventory	Not used	Not used	Not used	Not used
Pedrozo - Acuña (2017)	Phenomenological	Exposure	Floods	Not used	100	Not used	Not used	Not used
Pregnolato et al. (2017b)	Hybrid	Travel time increase	Floods	Rainfall- runoff model	3 climate change scenarios	Topological model of Ford et al. (2015)	Non declared	Vehicle speed – water depth model and depth threshold
Hackl et al. (2018)	Hybrid	Annual exceedance probability x Consequences = (1/T)(costs)	Floods Mudflow	Hydrological- Hydraulic model	2, 5, 10, 25, 50, 100, 250, 500, 1000, 2500, 5000, 10000	Assets Repairing Travel time w/BPR; Trip Losses Unsatisfied Vehicle operating costs	Deterministic	Theoretical Fragility models
Wang et al. (2020)	Hybrid	Travel time increase	Floods	Flood model + Global climate model	3 climate change scenarios.	Travel time	Multiagent microsimulation	Not used
van Ginkel et al. (2021)	Hybrid	Damage probability = hazard x exposure x vulnerability	Floods	Flood maps	10, 20, 50, 100, 200, 500,	Recovery	Not used	Damage curves: cost – water depth
Zhang and Alipur (2020)	Hybrid	Robustness index	Floods	Model not reported	500	Vehicle operating costs Opportunity loss costs	Not used	All-or- nothing Road or bridge closure in terms of water depth tolerance





Author	Risk	Model		Hazard			Vulnerability Mode	els
	Туре	Specification	Туре	Flood model	Return Periods (T, years)	Costs	Traffic assignment	Vulnerability
Zhang and Alipur (2022)	Hybrid	Annual exceedance probability x Consequences = (1/T)(costs)	Floods	Model Not reported	2, 5, 10, 25, 50, 100, 200, 500	Recovery cost Travel time Opportunity loss costs	Wardrop's equilibrium model	All-or- nothing Road or bridge closure in terms of water depth tolerance
Moghtadernejad et al. (2022)	Hybrid	Cost minimization with simulated annealing, genetic algorithm, particle swarm optimization	Runoff Floods Mudflow	Model Not reported	500	Assets Repairing Trips losses Travel time w/BPR Vehicle operating costs	ODM, 4STM and Optimization w/Franke-Wolf	Fragility models of Lam and Adey (2016) Identification of the most damaged road sections w/Scott et al. (2006) model.
Shahdani et al. (2022)	Hybrid	Travel time increase	Floods	Hydrological- Hydraulic model	20, 100, 1000	Not estimated	Traffic simulation	Vehicle speed – water depth threshold of Pyatkova et al. (2019)

3 Procedure of estimating the road network flooding risk

125 3.1 General description of the procedure

The result of the procedure is economic losses in terms of costs for road users of road networks affected by floods for return periods between two and 100 years. To estimate the losses, the procedure incorporates hydrological and hydraulic modeling to simulate flood conditions, which then inform road and bridge vulnerability, culminating in a traffic assignment model that estimates the resultant economic impacts.

Road vulnerability was estimated as a function of the probability of traffic interruption owing to flooding. The bridge vulnerability was calculated as the probability of scour exceedance. The exposure was obtained from overlapping flood maps and the road network under study. Flood maps were obtained using a combination of hydrological and hydraulic models for different return periods.

The indirect costs of flooding are estimated in terms of road user costs. These costs are the sum of fuel consumption and travel time costs. They were estimated under normal operating conditions of the road network and for restrained operations under different road flooding scenarios. Under normal conditions, road user costs are estimated by applying a traffic assignment model. The model assigns traffic to minimize the travel time of road users in an entire road network. Under restrained





conditions, fuel consumption and travel time increase owing to rerouting caused by the disabling of total or partial road sectors and bridges or by speed reduction during the flood.

140 The traffic assignment model was applied to estimate the fuel consumption, travel time, and costs for different flood scenarios. The difference in fuel consumption and travel time costs between normal and restricted operations was the net increase in the cost of the entire road network for each flood scenario. The traffic assignment model uses road and traffic data obtained from national road and traffic surveys conducted by road agencies. It also uses a travel time function that considers the capacity and traffic of different road types. The model was applied successively for each return period to obtain the cost-return period pairs 145 with which the loss model was prepared.

3.2 Workflow

Figure 1 shows the step-by-step procedure proposed for road network risk estimation, which comprises (1) hazard modeling (HMH), (2) road network exposure (RE), and (3) road network risk calculation (RM).

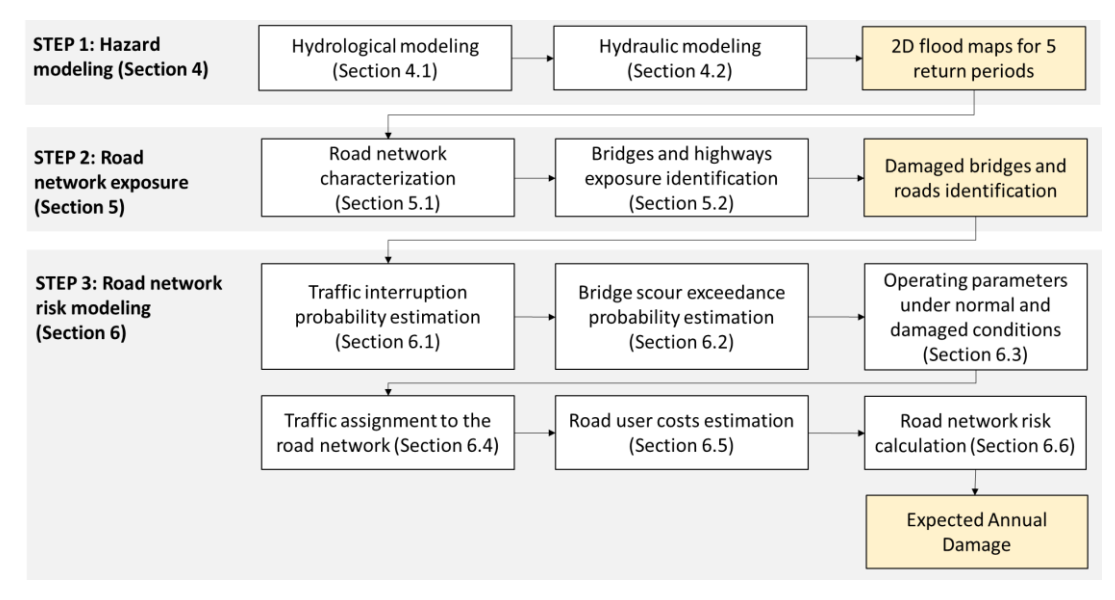


Figure 1: Procedure for calculating road network flooding risk.

The input data for the HMH module were as follows:

- Morphometric data: topography, river network, rainfall-contributing area, main channel length, and average slope
- Hydrological data: maximum rainfall in 24 h for a return period of 10 years and maximum annual discharge.
- Road network data: spatial representation of road links, nodes, and bridges; their physical characteristics, such as cross-155 section width, pavement type, and capacity; and operational characteristics, such as average speed, traffic volume, and vehicle traffic composition.

150

https://doi.org/10.5194/egusphere-2025-4016 Preprint. Discussion started: 10 November 2025

© Author(s) 2025. CC BY 4.0 License.



160

165

170

175

180



• In the HMH module (step 1), flood maps are obtained as follows: a) estimation of hydrographs at the entrance of each sub-watershed by hydrological modeling and b) spatial representation of flood by 2D hydraulic modeling for each return period. If discharge data are available, flood hydrographs are obtained by tracking floods in the daily maximum discharge registers. If discharge data are unavailable, a hydrograph can be obtained using locally calibrated rainfall-runoff models. The maps indicate the flood surfaces, heights, and flow velocities for different return periods.

In step 2 (RE), the flood-affected road network was identified by superimposing the flood maps for each return period on the road network map. The flood height was obtained for the flooded roads, and the water depth was estimated for all bridges. In Step 3 (RM module), the probability of traffic disruption was calculated for each vehicle class and return period using the model proposed by Contreras-Jara et al. (2018). Subsequently, the exceedance probability of scouring and its effect on capacity reduction were estimated for each bridge using the models of Chamorro et al. (2020). The RM module then identifies the road network characteristics and determines the traffic capacity and operating speed at each network link under normal and restrained operating conditions. Under normal operating conditions, no network links are physically affected by floods. In a restrained operation, one or more network links are partially or fully disabled owing to a flood, forcing traffic to reroute, or speed reduction. Restricted operating conditions in flooded links were assumed if the waterlogging probability exceeded a predetermined value. The circulation speed was calculated using the model proposed by Pregnolato et al. (2017). Finally, a traffic assignment model was applied under normal and restrained conditions. The speed, traffic volume, and travel time of each road network link are then determined. The road user cost is the sum of these costs per link and vehicle type. The total costs for the network under normal and retrained conditions are the sum of the road user costs of each link and vehicle type. The cost difference between normal and restrained conditions results in operational losses after flooding.

4 Study area

The study area is known as "Aconcagua Bajo" (LAB) (Figure 2). The watershed originates 4 km downstream of San Felipe City at the confluence of the Aconcagua and Putaendo Rivers. It belongs to the larger watershed of the Aconcagua River, located in the central zone of Chile between the coordinates [32-43'37.9" S, 70-46'09.21" W] and [32-55'21.9" S, 71-30'32.1" W].





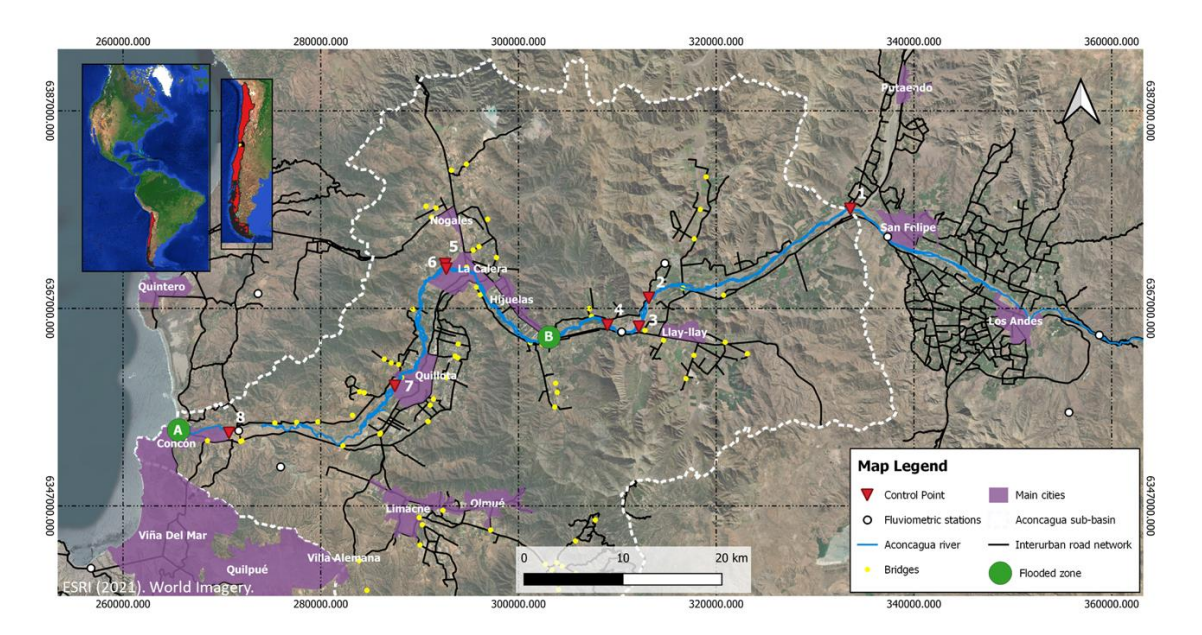


Figure 2: Location and general characteristics of the study area in the "Aconcagua Bajo" watershed.

The main watercourse of the LAB is the Aconcagua River, which is 152 km long and flows from the east to the west. The watershed has an area of 2,625 km² and an average flat slope between 160 and 200 m/km. It has a mixed pluvial-nival regime, a monthly average discharge between 20 and 50 m³/s, and a maximum rainfall in 24 h between 80 and 110 mm in a return period of 10 years (MOP, 2004; MOP, 2019a). The road network in the LAB is mainly linear and spatially located on the margins of the floodplains in the watershed. The road network comprises two multilane roads connecting the cities of Los Andes, La Calera, Quillota, Concon, and Viña del Mar, and a complementary network composed of two-way, two-lane rural roads. Two percent of the watershed land use is urban and 13% of the surface is used for forestry and agricultural activities. In addition, 35% of the land was wooded, 32% was grassland, 4% was water bodies, and the remaining 14% was un-vegetated. Industrial activity is present in the cities mentioned, and agricultural use occurs in rural areas adjacent to the watercourses (MOP, 2004).

5. Hazard modeling

185

190

195

5.1. Hydrological modeling

Hydrological modeling was performed using a rainfall-runoff model calibrated for Chile by Verni and King (1977) in watersheds between 20 and 10,000 km², with return periods of less than 100 years and a mixed nival-pluvial regime. In the case study, the watersheds had areas between 1638 and 3860 km², and modeling was performed for return periods of up to 100 years; therefore, the model of Verni and King (1977) is applicable to the situation represented in the case study.



215



Regarding the input parameters used, the topography was obtained from the ALOS PALSAR digital elevation model developed by the Japanese Aerospace Exploration Agency in its 2011 mission (JAXA). The resolution was 12.5x12.5 m. Hydrographic data were obtained from the Chilean Ministry of National Land (MOP, 2017). Geomorphological data of the watershed were obtained from post-process topography, hydrographic information, and the contributing areas. The model of Verni and King (1977) used as input data the maximum rainfall in 24 h for a return period of 10 years (P₂₄¹⁰, mm), watershed area, duration factors, and return period factor to adjust the maximum flow in every watershed without fluviometric data. Parameter P₂₄¹⁰ was obtained from the online Hydrometric System of the General Directorate of Waters of the Ministry of Public Works of Chile (MOP 2019a). All the data are freely accessible.

Hydrologic modeling was performed using a rainfall-runoff analysis owing to the lack of flow information for the entire Aconcagua Basin. For this purpose, flood routing was performed by dividing the basin into eight sub-basins, each with its own attributes and precipitation data. In addition, eight checkpoints (PC) were set at the end of each sub-watershed, including the main channel of the Aconcagua River (Figure 2). Each PC had specific input data depending on the runoff-contributing area (Ap). Table 2 shows the input data of each PCi.

As the first step of the modeling, using the model of Verni and King (1977) as a function of the parameters described in Table 2, the flow rates for return periods of 2, 10, 25, 50, and 100 years were obtained (Table 4). Then, based on the parameters in Table 3, the synthetic unit hydrograph of each sub-basin was obtained and adjusted according to the flow obtained using the Verni and King (1977) model and the time of concentration "tc" of each sub-basin. The criterion used was that the concentration time was equal to the time required to reach the peak value. As a result of hydrologic modeling, five hydrographs for each return period were obtained for the eight sub-basins.

Table 2: Input data for hydrological model.

Input data	PC_1	PC ₂	PC ₃	PC ₄	PC ₅	PC ₆	PC ₇	PC ₈
Ap (km ²)	1636.8	2154.3	313.4	574.2	2452.7	418.5	2983.2	3860.4
Ls (km)	63.5	89.9	30.1	96.4	115.1	22.3	130.7	152.2
Lg (km)	17.0	33.1	12.2	43.0	43.7	10.2	44.8	52.6
S (m/m)	0.4	0.4	0.4	0.3	0.4	0.4	0.4	0.4
D (km)	5.3	4.3	1.9	3.6	4.3	2.1	4.4	4.5
tc (h)	4.2	6.8	2.6	8.0	9.1	1.8	10.4	12.3
P ₂₄ (mm)	80.0	83.3	80.0	120.0	88.2	100.0	100.0	110.0

Ap: basin area; Ls: length of the channel upstream of PC_i; Lg: distance between the center of gravity of the basin and the location of the PC_i; S: average slope of each basin obtained from the digital elevation model (DEM) using the QGIS Slope tool (QGIS Development Team, 2021); D: maximum height difference between the highest point of the basin and the PC_i; to: time of concentration in each virtual sub-basin; P₂₄¹⁰: maximum rainfall in 24 h for a 10-years return period (T).







225

Table 3: Synthetic unit hydrograph parameters.

Parameter	PC_1	PC_2	PC ₃	PC ₄	PC ₅	PC ₆	PC ₇	PC ₈
$t_{p}(h)$	7.52	11.57	4.73	11.09	14.64	4.01	15.56	17.87
$t_b(h)$	27.28	38.60	18.77	37.30	46.64	16.44	48.98	54.76
$q_p (m^3/s/km^2)x10^{-3}$	28.93	20.53	41.87	21.24	17.02	47.75	16.22	14.53

t_p: time to peak discharge; t_b: base time; q_p: peak discharge.

Table 4: Flow rates per return period of each hydrograph at checkpoint.

PC _i		Q(T) (m ³ /s)								
	T = 2 years	T = 10 years	T = 25 years	T = 50 years	T= 100 years					
PC ₁	420.3	676.7	822.1	946.2	1066.2					
PC_2	562.8	906.1	1100.8	1267.0	1427.6					
PC_3	11.8	64.5	96.9	138.2	185.8					
PC_4	276.4	445.0	540.8	622.3	701.2					
PC_5	677.3	1090.2	1324.6	1524.5	1717.7					
PC_6	778.0	1252.3	1521.5	1751.2	1974.2					
PC_7	940.2	1513.5	1838.7	2116.3	2384.6					
PC ₈	542.2	2137.0	2596.4	2988.3	3367.1					

5.2. Hydraulic modeling

230 HEC-RAS 2D software (USACE, 2016) was used for hydraulic modeling. Flood hydrographs were estimated using hydrological modeling for each return period. The topography of the study area and the Manning roughness coefficients for each sub-watershed were used as input data in the HEC-RAS 2D model. The same return period was simulated for the entire Aconcagua River Basin. The floodable area was identified and assigned roughness and slope, and the input and output hydrographs were obtained from the DEM used for hydrologic modeling. These data were used to estimate the flood surface, 235 flood height, and flow depth of the bridges, roads, and riverbanks in the area. The hydraulic model output represented the maximum flood depth for each return period in the eight sub-watersheds. Figure 3 and Figure 4 show the flood surface and maximum flood depth in zones A and B, Figure 2.

The significant scarcity of comprehensive real-time precipitation data across the entire Aconcagua Basin, with reliable records limited to only two stations situated in the headwaters, precludes the direct use of actual rainfall for the comprehensive hydraulic model calibration and validation. Consequently, the Verni and King (1977) hydrological model was employed to estimate the discharge. Full model calibration or validation using actual distributed rainfall was not feasible under these data constraints; rather, the estimated flows were verified against limited fluviometric station data.



245

250

255

260

265



Data from two available fluviometric stations (San Felipe and Llayllay) were used to verify discharge over a 25-year return period. However, insufficient discharge and correspondingly low water height records at these stations precluded the validation of simulated flows. Consequently, verification must be conducted at specific locations using sufficient data. Therefore, PC1 can only be verified for a 25-year return period. The maximum measured discharge at this control point was 800 m³/s, which was associated with T=25 years (Alvarez-Garreton et al., 2018). The discharge modeled for this return period was 822 m³/s, which was 3% greater than the measured value.

Similarly, the specific discharge reported by Alvarez-Garreton et al. (2018) was 0.153 m³/s/km², and the model was 0.147 m³/s/km², which is 4% less than the former. Therefore, the modeled flows were assumed to be valid for 25 years. In addition, water height data were compared with data from an existing fluviometric station in the Lower Aconcagua watershed. The data from the fluviometric station showed water heights between 4.4 and 4.8 m for a maximum discharge of 800 m³/s. The modeled water height resulted in values between 4.7 and 5.2 m for a return period of 25 years. The maximum difference was 8%.

6. Road network exposure

6.1. Road network characterization

The road network under study is in the ancient floodplain of the Aconcagua River, with the main road network on both banks of the river. Road networks near towns and cities have subnetworks that provide accessibility between towns, farms, and main roads. These subnetworks have a geometric design standard that is lower than that of the main route of the network.

The road network in the study area and its specific characteristics were obtained from the geodatabase of roads of the Chilean Ministry of Public Works (MOP 2020a, 2020b). The roads were classified into three categories according to the average speed and road capacity: multilane, two-way, and two-lane Class 1 roads; and two-way and two-lane Class 2 roads (see Table 6). The principal road network consisted of 307 km of multilane roads and 1516 km of two-way, two-lane Class 1 and Class 2 roads, all of which were paved. On multilane roads, each carriageway cross-section consists of two lanes (3.5 m wide each), a 2.5 m-wide shoulder, and a 6 m wide median. On two-way, two-lane roads, the cross-section consists of one lane per traveled way, a lane width of 3.5 m, and shoulders of 1.5 m.

The road network has 79 bridges, with lengths ranging between 10 and 530 m. Nine bridges cross the main watershed river (Aconcagua River). Of these, 75% are one-span bridges, and the remaining 25% are two or more span bridges. The annual average daily traffic (AADT) and its composition were estimated using the traffic database of the Chilean Ministry of Public Works (MOP, 2020c) available online. On multilane roads, the AADT varied between 4,670 and 17,670 vehicles/day-year. On Class 1 roads, the AADT varied between 605 and 9,449 vehicles/day-year. On Class 2 roads, the AADT varied between

On Class 1 roads, the AADT varied between 605 and 9,449 vehicles/day-year. On Class 2 roads, the AADT varied between 1,105 and 8,015 vehicles/day-year.





6.2. Bridges and highways exposure identification

The road network was overlaid on the flood maps obtained from the hydrological-hydraulic simulation to identify flood-affected road infrastructure. The flooded road segments, lengths, and maximum flood depths were identified for each return period. Bridges with a probability of scour design exceedance greater than zero were also identified. Table 5 summarizes the results. Figure 3 and Figure 4 highlight the flood surface and water depth in zones A and B in Figure 2.

Table 5: Flood-affected roads and bridges for each return period

R	oad Element			Return period (year	rs)	
		2	10	25	50	100
Multilane	# Sections	2	4	4	4	4
	$H_{av}\left(m\right)$	0.45	1.25	1.57	1.75	2.18
	L (m)	1846	3182	3182	3182	3182
Two-way	# Sections	5	9	10	10	10
Two-lane	$H_{av}\left(m\right)$	1.23	1.25	1.43	1.73	2.35
Class 1	L (m)	960	3426	3512	3512	3512
Two-way	# Sections	1	2	2	2	2
Two-lane	$H_{av}\left(m\right)$	0.02	0.75	1.6	1.7	3.7
Class 2	L (m)	439	960	960	960	960
1-span	# bridges	0	0	0	0	0
Bridge	Exceedance	0	0	0	0	0
	Probability					
+1-span	# bridges	0	1	2	3	3
Bridges	Exceedance	0	0.73	[0.07-0.83]	[0.07-0.83]	[0.08-0.90]
	Probability					





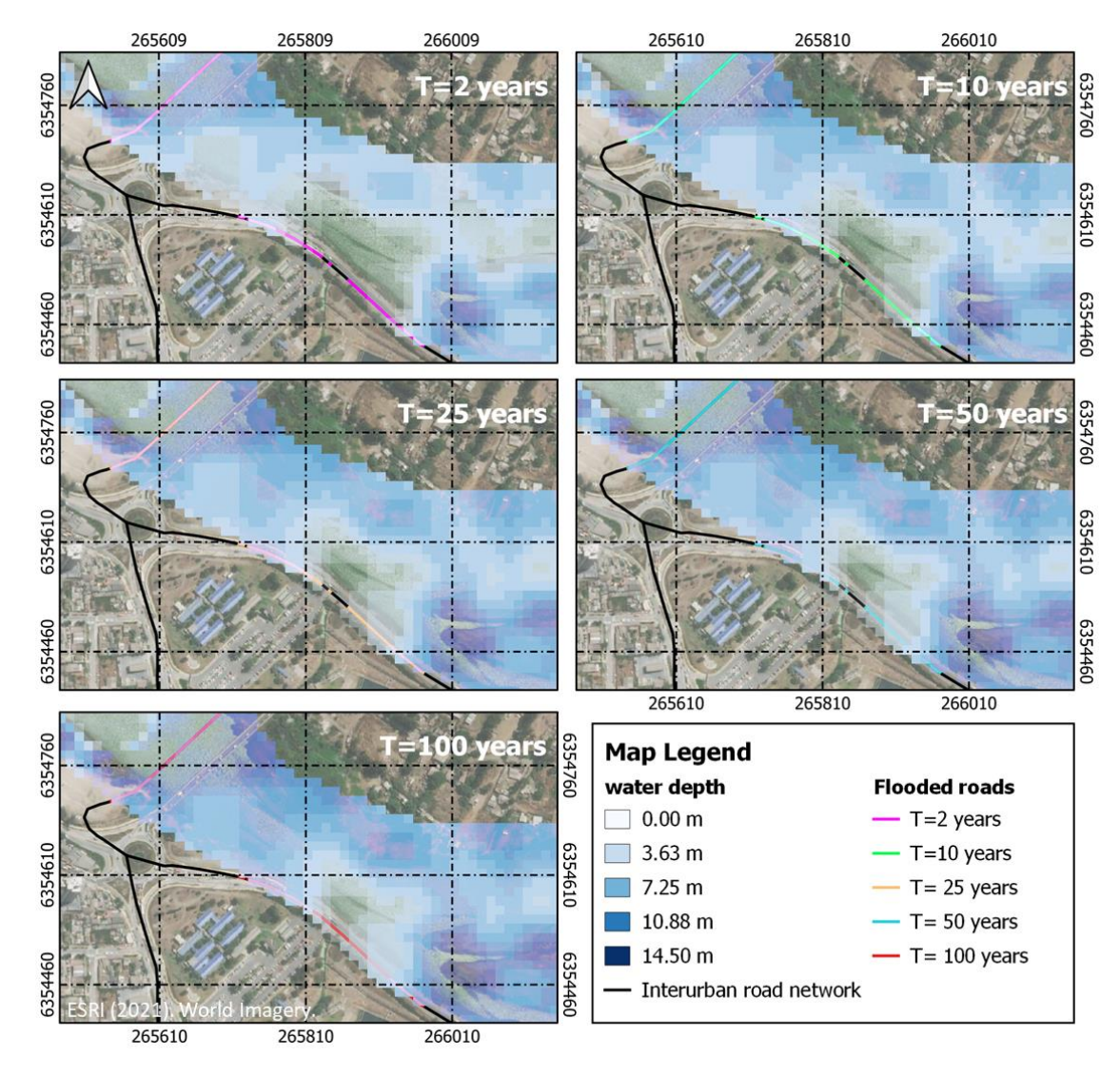


Figure 3: Zone A: Flooded roads and bridges, their lengths, and flood height.





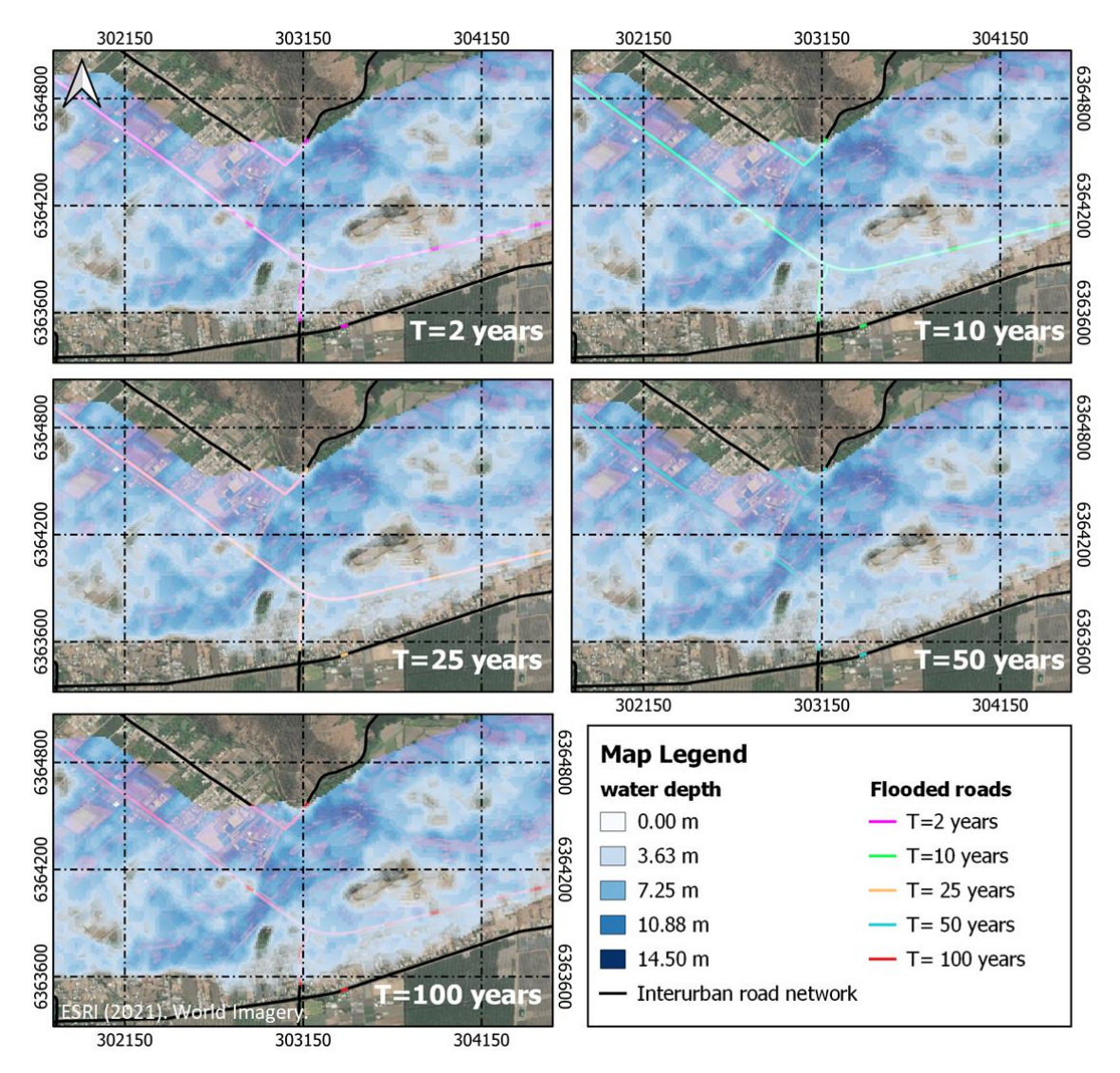


Figure 4: Zone B: Flooded roads and bridges, their lengths and flood heights.

For the range of analyzed return periods, the following patterns were identified: a) between 2 two to four sections of flooded multilane roads, with a total affected length of 1.8 to 3.2 km and water heights between 0.5 and 2.2 m; b) five to ten flooded sections of Class 1 roads with a total affected length between 960 and 3512 m, and flood heights between 1.2 and 2.3 m; and c) up to two flooded sections of Class 2 roads with a total affected length between 439 and 960 m and flood heights up to 3.7 m. In addition, between one and three bridges with two or more spans affected by flooding were identified, mainly belonging to the multilane and Class 1 two-way two-lane roads.





7. Road network risk modeling

290 7.1. Traffic interruption probability estimation

The traffic interruption probability model for flooding is given by Eqs. (5) and (6) for light (P_{int-light}) and heavy (P_{int-heavy}) vehicles, respectively, were used to estimate road vulnerability. Contreras-Jara (2018) calibrated Eq. (5) and Eq. (6) for Chilean conditions. The model estimates the traffic interruption probability with respect to the flood height (h, m).

$$P_{int-light} = 1 - e^{-79.829h^{5.223}}$$
 (5)

$$P_{\text{int-heavy}} = 1 - e^{-0.137 h^{12.917}}$$
 (6)

7.2. Bridge scour exceedance probability estimation

295 The bridge vulnerability was calculated using the model proposed by Contreras-Jara (2023). This model estimates the scour exceedance probability of bridges with one or more spans exposed to local scouring. The exceedance probability was estimated based on the water depth and return period.

7.3 Operating parameters under normal and restricted traffic conditions

For each return period, the probability obtained according to Sections 6.1 and 6.2 sets a limit on the water height and determines whether each link operates under normal and restricted conditions. In the flooded links, the limit values of $P_{int-light}$ and $P_{int-light}$ of 15% were defined. According to Eqs. In Equations (5) and (6), the flood height limits for light and heavy traffic are h = 0.3 m and h = 1.0 m, respectively. The traffic conditions were as follows:

- If h < 0.3 m, light and heavy traffic operate under restricted conditions.
- If 0.3 m < h < 1.0 m, light traffic is interrupted, and rerouting is required. Heavy traffic operates under restricted conditions.
- If h > 1.0 m, light and heavy traffic were interrupted. Re-routing is needed.

Table 6 lists the parameters under normal and restricted conditions for each road type and vehicle class.

Table 6: Operating parameters under normal and restricted conditions

Operating	Road category	Road asset	Vehicle	Average	Capacity	Pavement
Condition			class	travel speed (km/h)	(pcu/h/lane)	Roughness (m/km)
Normal	Multilane	Roads and bridges	All	100	2200	2.0
	Two-way two-lane Class 1	Roads and bridges	All	70	1800	5.0



320



Operating	Road category	Road asset	Vehicle	Average	Capacity	Pavement
Condition			class	travel speed	(pcu/h/lane)	Roughness
				(km/h)		(m/km)
	Two-way two-lane	Road and	All	50	1400	5.0
	Class 2	bridges				
Restricted	All road's categories	Roads	Light	10	2200	10.0
			Heavy	10	1800	10.0
			All	0	1400	10.0
	Multilane	Bridges	All	100	2200	2.0
			All	30	1760	10.0
			All	0		10.0
	Two-way two-lane	Bridges	All	70	1800	5.0
	Class 1		All	30	1440	10.0
			All	0		10.0
	Two-way two-lane	Bridges	All	50	1400	5.0
	Class 2		All	30	1120	10.0
			All	0		10.0

The design speed and highway capacities under normal operation were obtained from MOP (2019b). Under restricted operating conditions, the traffic speed on roads and bridges is reduced. On flooded roads, the speed was calculated using the model calibrated by Pregnolato et al. (2017a, b) (Eq. (7)), which estimates the speed limit of light vehicles in the event of flooding (V_{lim}, km/h) from the height of the flood on the road (h_R, mm). For larger vehicles, a height limit of 1000 mm was used to estimate V_{lim}.

$$V_{lim} = \begin{cases} 0.0009h_R^2 - 0.5529h_R + 86.9448 & ; & h_R \le 300 \text{ mm} \\ 0 & ; & h_R > 300 \text{ mm} \end{cases} \tag{7}$$

For bridges, the operating speed was set to 20 km/h when the scour design exceedance probability was 0.3 and 0.6. The total traffic disruption was assumed for exceedance probabilities higher than 0.6, with an operating speed of 0 km/h.

We assumed that the capacity of the flooded roads remained constant at different flood heights and that only the speed changed, according to the model proposed by Pregnolato et al. (2017a). Above these values, the capacity is zero owing to traffic interruptions. For bridges, it was assumed that scour probabilities between 0.3 and 0.6 are in such a state of damage that traffic and structural capacity are reduced (Hack et al., 2017). Under these conditions, the reduction in bridge capacity was estimated to be 20%, assuming normal conditions for vehicles (Bocchini and Frangopol, 2018). For exceedance probabilities greater than 0.6, traffic interruption was assumed; therefore, the traffic and structural capacities of the bridge were considered zero.



335



7.4 Traffic assignment to the road network

The traffic assignment model applied in this study sought to optimize traffic flow across the network, minimizing travel time under both normal and flood-affected conditions. This model leverages national traffic data and road network characteristics to simulate how floods reroute traffic and increase the user costs.

The network was built with 154 links and 129 nodes using GIS. Six modeling networks were considered, one for each return period. The operational physical attributes for the normal and restricted operating conditions were assigned to each link according to the following rules:

- Physical attributes under normal conditions, road class, and length of each link.
- Physical attributes under restricted conditions, road class, length of each link, flooded segment, flood height, and the link to which the flooded segment belongs.
 - Operating attributes under normal and restricted conditions: According to Table 6.

The traffic assignment model (TAM) of Beckmann et al. (1955), extended by Nie et al. (2004), was used. TAM assigns traffic to a road network "G" composed of "N" nodes and "A" links, thereby minimizing the total travel time. To this end, the optimization problem in Eq. (8) to Eq. (13) was solved using the algorithm proposed by Kumar (2019).

$$\min \sum_{a \in A} \int_{0}^{f_{a}} t_{a}(x) dx \tag{8}$$

In Eq. (8), where "a" represents each link of network "G," " f_a " is the traffic in link "a," and " t_a " is the total travel time in link "a," calculated using Eq. (13). The "a" links of the network "G" are obtained from national road surveys, with which a connected network is prepared. The traffic " f_a " is obtained from national traffic surveys and is generally expressed as average annual daily traffic (AADT). The restrictions on the optimization model are as follows (Bar-Gera, 2002; Nie et al., 2004).

Total vehicle flows equal to the demand for each origindestination: $\sum_{p \in P_{W}} h_{p} = T_{W} \quad ; \quad w \in W$ (9)

Traffic in the link is the sum of the flows of all routes that use that link:

$$f_a = \sum_{p \in P_w} \delta_{ap} h_p \quad ; \quad a \in A$$
 (10)

No traffic negativity on route "p":

$$h_{p} \ge 0 \ ; p \in P_{w} \tag{11}$$

No negativity of traffic in the link "a":

$$f_a \ge 0$$
; $a \in A$ (12)

$$t_a = t_a^0 \left[1 + \alpha \left(\frac{f_a}{c_a} \right)^{\beta} \right] \tag{13}$$

In Eq. (9) to Eq. (12), where "w" is a travels origin-destination (O-D) pair; "W" is the set of all O-D pairs in the "G" network; "P" represents all possible routes in the road network. It can be obtained from an O-D survey or zoning of the study area, and traffic data from national surveys estimate the traffic (h_p) at each link "a" that connects each zone. "P_w" is the set of available



350

355



routes connecting the O-D pair "w" which are obtained from the network "G"; " T_w " is the traffic in the O-D pair "w" that are obtained from the network "G". " h_p " is the traffic in route "p"; and " δ_{ap} " is a dummy coefficient ($\delta_{ap} = 1$ if the link "a" belongs to the route "p"; otherwise, $\delta_{ap} = 0$). In Eq. (13), " t_a " is the travel time in the link "a" (h); " t_a 0" is the travel time (h) of link "a" in free-flow condition, which is obtained by dividing the length of each link by the average travel speed or by the design speed. " c_a " is the capacity of link "a" ($p_{cu}/h/lane$), which can be obtained from TRB (2016). Generally, the capacity of two-lane rural roads ranges between 1400 and 1800 ($p_{cu}/h/lane$), and multilane rural roads vary between 2000 and 2200 $p_{cu}/h/lane$. These variations depend on whether the terrain is flat, rolling, or mountainous. The parameters α and β were obtained from the TRB (2010 and 2016) (α =1.5 and β =5 for multilane and Class 1 roads; α =1.2 and β =5 for Class 2 roads).

Traffic data were obtained from the National Traffic Survey, issued for two years each, and are freely available on the Chilean Ministry of Public Works website (MOP, 2020c). These data were used to estimate the origin destination matrix. After applying TAM, the modeled traffic was compared with the existing flows in the road network. Figure 5 shows the correlation between the modeled and actual traffic data. Traffic was expressed as passenger car units per hour per lane (pcu/h/lane). The outlier data points represent traffic in the cities of Hijuelas (Point 1) and Limache (Points 2 and 3).

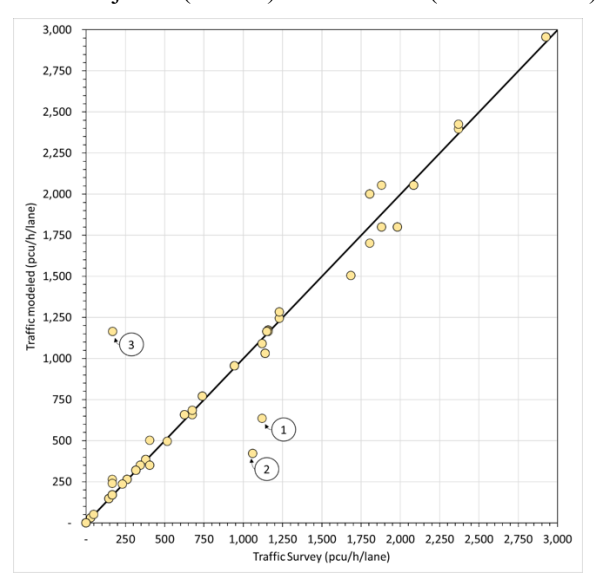


Figure 5: Traffic assignment model calibration results in normal operating condition

7.5 Estimating Road user costs

The road user cost (RUC) corresponds to the sum of the travel time (TTC) and fuel consumption (FCC) costs, as expressed in Eq. (14).

$$RUC = FCC + TTC = \left[\sum_{a=1}^{A} \sum_{v=1}^{V_a} d_a FC_v f_v + \sum_{v=1}^{V} t_v s_v \right]$$
(14)



365



In Eq. (14), where "V" is the traffic assigned; "V_a" is all vehicles assigned in the link "a"; "d_a" is the length of the link "a" (km); "FC_v" is the fuel consumption of vehicle "v" (liters/km); "f_v" corresponds to the unit cost of fuel for vehicle "v" (US\$/liter); "t_v" corresponds to the travel time of vehicle "v" (h) obtained from the TAM; "s_v" is the unit cost of the time for vehicle "v" (US\$/h). The unit fuel consumptions of light vehicles (FC_{lv}, ml/vehicle-km) and heavy vehicles (FC_{hv}, ml/vehicle-km) were calculated using Eqs. (15) and (16), depending on the pavement roughness (IRI, m/km) and operating speed (OS, km/h). The fuel consumption models in Eqs. (15) and (16) were obtained from the HDM-4 model calibration developed by the Chilean Ministry of Public Works (MOP, 2018).

$$FC_{lv} = (1255.7 - 1.7735 \text{ IRI})OS^{-(0.543 - 0.0009 \text{IRI})}$$
(15)

$$FC_{hv} = (8308.2 - 10.085 \text{ IRI})OS^{-(0.3048 - 0.0004 \text{IRI})}$$
(16)

A travel time unit cost of US\$ 18.6/h/vehicle for light vehicles and US\$ 64.0/h/vehicle for heavy vehicles were used. The unit fuel costs are US\$ 0.5/liter/vehicle and US\$ 0.6/liter/vehicle for light and heavy vehicles, respectively (MDS, 2020).

370 7.6. Road network risk calculation

The expected user cost is considered a proxy for flood risk in road networks. The total expected user costs (EUC, in US\$/year) in the network are obtained using Eq. (17), where T_1 – T_5 are the return periods of 100, 50, 25, 10, 5, and 2 years, respectively, and S_1 – S_5 are the expected user costs (EUC) for each return period, estimated using Eq. (14), which represents the area under the curve, as shown in Figure 6.

$$EUC = \frac{1}{T_1}S_1 + \left[\frac{1}{T_2} - \frac{1}{T_1}\right]\frac{S_1 + S_2}{2} + \left[\frac{1}{T_3} - \frac{1}{T_2}\right]\frac{S_2 + S_3}{2} + \left[\frac{1}{T_4} - \frac{1}{T_3}\right]\frac{S_3 + S_4}{2} + \left[\frac{1}{T_5} - \frac{1}{T_4}\right]\frac{S_4 + S_5}{2}$$

$$\tag{17}$$

375 The total EUC obtained was 5.700.000 US\$/year. This cost represents the additional travel time and fuel consumption costs owing to vehicle rerouting in the network caused by flooded road segments, bridge closures, or heavy traffic restrictions on damaged or weakened bridges in the road network under consideration. The accuracy of the estimated EUC increased when additional floods with different return periods were added to Eq. (17). Figure 6 shows the expected losses in terms of road user costs of the network and each return period.



385

390

395



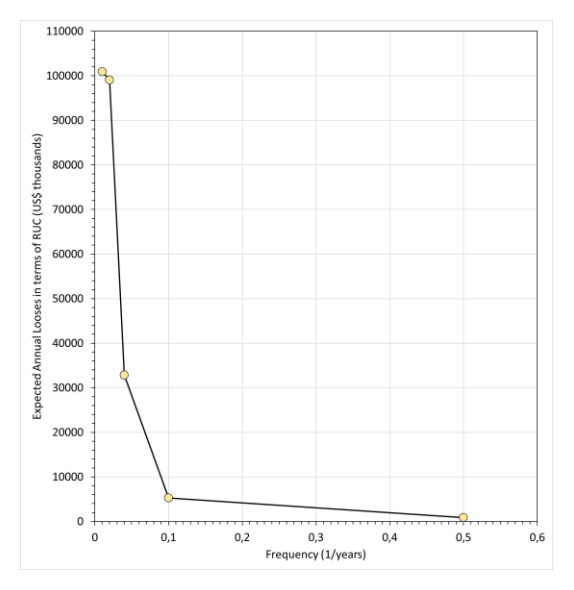


Figure 6: Expected annual losses in terms of road user cost for each return period

Figure 6 shows the estimated benefits of flood abatement on road networks. According to Penning-Rowsell and Green (2000), if abatement measures are set for a return period of 100 years, then the expected annual benefits are approximately equal to the EUC obtained in this case study. However, to estimate the net benefit, it is necessary to assess higher return periods, estimate the abatement costs at each bridge and road segment affected by floods, and apply the TAM to recalculate the road user and fuel consumption costs for new rerouting schemes. In addition, shows the avoided costs when implementing risk abatement measures on roads and bridges to ensure the operational continuity of the road network after flooding. The results also allow for the assessment of the benefits of keeping roads open after a flood to permit evacuation and attend to people affected by floods.

7.7. Results discussion

The flow rates estimated by the Verni and King (1977) model were compared with the available data. This verification indicated that the flows estimated with this model, compared with those available from the PC1 fluviometric station (the only spot check located at the head of the Aconcagua Basin), overestimated the 25-year return period by 3%. This discrepancy subsequently affected the hydraulic modeling results, resulting in an 8% increase in the estimated flood extent and maximum water height compared with the locally reported values. Such variations may stem from multiple factors, including hydrological model calibration, input topographic data quality, and roughness coefficients. Nonetheless, the obtained values were acceptable for regional-scale simulations.

The vulnerability estimation of roads and bridges was conducted using models calibrated for Chile, considering the characteristics of the local vehicle fleet and the climatic conditions. Therefore, the results for the probabilities of disruption

21



405

410

415

420

425

430



and scour exceedance were suitable for this case study. However, it is crucial to acknowledge that these results are conditioned by the quality of the input data, particularly the digital elevation model and flood map used for each return period.

The traffic modeling results were validated using data from the Chilean Ministry of Public Works. The traffic model calibrated for normal operating conditions demonstrated a solid statistical fit with a coefficient of determination of R²=0.98, underscoring its accuracy and representativeness. However, this calibration was not performed under restrained traffic conditions after floods, because of unreliable traffic data. Calibration under these conditions requires counting traffic in extensive road networks before and immediately after floods, which is very difficult to achieve.

EUC estimation implies the combination of datasets, models, and procedures from different origins, which, when combined, introduces errors that propagate throughout the process and affect the results of the study. This study did not include a sensitivity assessment or error identification. However, this type of analysis can be performed using procedures such as those used by Allen et al. (2022), who assessed the sensitivity of the seismic risk assessment of road networks and identified the effect of different error sources on the EUC results.

EUC estimation relies on the following data inputs: digital elevation models, traffic and road network data, and hydrological data (such as discharge and water height). Among these, the resolution of the DEM is a determinant of the accuracy of flood extent and water level modeling. The resolution of the DEM can directly impact vulnerability quantification, as a coarser grid (e.g., 12.5×12.5 m) may identify more potentially affected road assets owing to less detailed terrain and channel bathymetry, leading to potentially overestimated flood extents and depths. Although such a DEM is suitable for preliminary analyses to pinpoint potential flood hotspots, transitioning to a higher resolution (e.g., 5 m ×5 m or 1 m ×1 m) is crucial for a more accurate assessment of vulnerability and, consequently, more reliable indirect cost estimations. This finer resolution allows for detailed site-specific studies in identified high-risk zones, enabling a more precise analysis of the impacts, especially considering that infrastructure dimensions, such as road lane widths (typically 3.5 m), are better represented, leading to a more accurate risk profile for specific assets. Discharge and water height data are required to calibrate the hydrological and hydraulic models. However, these data are not always available in terms of their quantity or quality. This situation arises in the studied basin, where only two stations in the basin headwaters provided sufficient data for analysis. Consequently, Verni and King's (1977) hydrological model calibrated for Chile was used. The model relies on the maximum precipitation isohyets to estimate flows.

However, the results obtained by the model were generally more significant than the data available for validation, which may have propagated errors in downstream flow modeling and, consequently, in flood map simulation.

Regarding hydraulic simulation, it is important to note that the flood map representation assumes a time-less scenario, graphically displaying only the maximum depth obtained from the simulation for each return period. Consequently, the model does not consider the temporal dynamics of flooded areas, including their appearance and disappearance over time, which can significantly affect traffic assignment.

Other aspects affecting the results were road and bridge vulnerability and the RUC models. Both models depend on local conditions and infrastructure design, which are based on design standards. Therefore, models from the literature are not



460



recommended for this type of analysis. This study used previously calibrated models for Chilean conditions to represent vulnerability and RUC.

The traffic assignment model was calibrated using the traffic data provided by the Ministry of Public Works of Chile under normal conditions. The calibration assumes that the origin destination does not change after the flooding. In this case, the only problem is traffic reassignment owing to the inability of flooded links to the road network. We also assume that there is no avoided travel, which can reduce the travel demand. Several authors recognize both assumptions; however, to date, no procedures exist that allow these effects on travel matrices.

Future research should focus on enhancing hydraulic modeling by moving beyond the current reliance on static flood maps, which typically represent only the maximum inundation depths. For example, this study assumed a constant flood duration of two hours. However, the development of dynamic models that can simulate the complete temporal evolution of flood events, including their initiation, duration, and recession, is crucial. Such advancements, even when utilizing a DEM of the same resolution, would enable a more qualified representation, differentiating between areas experiencing brief transient inundation and those subjected to prolonged periods of significant water depth. This dynamic perspective reveals that the vulnerability of road assets is not static but varies over the duration of an event. Consequently, traffic reassignment also becomes a dynamic process as network accessibility changes over time. This, in turn, would require corresponding improvements in traffic modeling to accurately capture and respond to this temporal variability in flood impacts and network conditions, thereby providing a more realistic understanding of overall system resilience.

Future research should focus on enhancing hydraulic modeling by moving beyond static flood maps that only represent the maximum inundation depths. The development of dynamic models that can simulate the temporal evolution of flood events, including their initiation, duration, and recession, is thus crucial. This advancement provides a more realistic understanding of how changing flood conditions affect traffic assignments and infrastructure vulnerabilities over time. In addition, addressing the significant gap in post-flood traffic data is of paramount importance. Current traffic models calibrated for normal conditions do not reflect post-disaster travel behavior; therefore, research is needed to establish reliable methodologies for collecting traffic data immediately following floods and to develop models that incorporate behavioral changes, such as trip avoidance or altered destinations.

Furthermore, given that Expected User Cost (EUC) estimation integrates outputs from sequential hydrological, hydraulic, vulnerability, and traffic models, understanding the propagation of uncertainties is vital. Errors introduced at any stage can cascade through the modeling chain and affect the final results. A critical area for investigation is the implementation of a comprehensive sensitivity analysis, similar to the approach employed by Allen et al. (2022), which covers the entire workflow. Such an analysis would identify the most influential parameters and data sources contributing to uncertainty and quantify how these errors propagate and impact the final EUC estimation, thereby strengthening the reliability of the risk assessment.





8. Conclusions

475

480

485

490

This study presents a method for estimating the expected user cost of a network affected by floods in terms of the return period and the costs involved in traffic rerouting owing to total or partial traffic interruption of roads and bridges. This method was applied to a case study of the road network of the "Aconcagua Bajo" watershed in central Chile. Flood hydrographs were generated using rainfall-runoff models calibrated for Chile. An open-source digital elevation model and traffic assignment model were also used. This study contributes to the existing literature by providing a comprehensive model that integrates hydrological-hydraulic analysis with road and bridge vulnerability assessments to estimate the EUC, a perspective that has not been thoroughly explored in previous studies.

The effects of floods on bridges and roads were analyzed, mainly because the road network is located on flat ground without cut slopes and embankments of significant heights in the area's natural terrain. However, analyzing the hydrometeorological hazards on road networks located on undulating or mountainous terrain requires including the effects of slopes, sliding slopes, debris flows, and more detailed digital elevation models than the one used. Furthermore, vulnerability and traffic interruption models must be considered natural hazards in steep or undulating terrains.

The traffic assignment was made considering that the origin-destination matrix was not modified by the effect of the modeled flood owing to its duration. An important aspect of future research is the analysis of the effect of flood road interruptions on non-travel decisions and their costs, as well as the modeling of traffic reassignment from flood onset to lowering water levels to normal values. Such research requires a dynamic traffic assignment model and in-depth analysis of how the travel matrix evolves during floods.

The expected user cost was aggregated on the network because the traffic assignment model does not identify the proportion of traffic that reroutes from one link to another in the road network or to which link it reroutes. Resolving this situation requires a traffic allocation model using an agent-based microsimulation model that enables the identification of individual behavior patterns in the network and the calculation of the risk level per link.

Network redundancy refers to the existence of more than two links connecting two nodes or origin-destination pairs. Redundancy exists if the links are similar in length, platform materials, traffic capacity, and bridges without load restrictions, and satisfy topological conditions based on centrality measures, such as betweenness or closeness. If these conditions are satisfied, two or more links provide redundancy to the road network. In contrast, a road network is non-redundant if the links are significantly different. Under this framework, the lack of redundancy reduces the possibility of traffic rerouting when a flood partially or totally interrupts a link, thereby increasing the travel time in the road network and risk. A detailed analysis of this effect enables decision makers to identify the investments needed in specific road network links to increase redundancy. However, this aspect of road networks was not examined in this study, which offers a research opportunity to improve the flood risk of road networks in the future.

The proposed method integrates the existing procedures to estimate hazards, traffic assignments, and road user costs. This method can be applied directly to other watersheds by considering local parameters. Hydrological-hydraulic models include

https://doi.org/10.5194/egusphere-2025-4016 Preprint. Discussion started: 10 November 2025

© Author(s) 2025. CC BY 4.0 License.



500

505

515

EGUsphere Preprint repository

local parameters and digital terrain models (DTMs). The traffic assignment algorithm depends only on road network properties, traffic data, and origin-destination matrices that can be estimated locally. The road-user cost parameters were obtained from the literature. Only models that estimate traffic interruption and scour exceedance probability must be locally developed and calibrated for each bridge. Therefore, considering local conditions, this procedure can be easily applied to other study areas in the future. The main weakness of hydrological-hydraulic issues is data availability, which depends on the availability and number of stations for measuring discharge and height over a significant period. Similarly, the availability of detailed landuse information in the watershed is required to estimate the concentration time comprehensively. Regarding traffic, the main challenge is dealing with changes in origin-destination travel, travel not carried out, and the differentiated effect on cargo and passenger travel.

This study did not examine the effect of the lack of redundancy on risk valuation, considering the road network as input data. However, we expect to assess the impact of increasing or reducing alternative routes on risk in future studies. Another relevant challenge is the establishment of error propagation throughout the procedure. This novel research field requires the development of more reliable risk estimations by identifying sources of uncertainty and their propagation.

510 Data availability

All raw data can be provided by the corresponding authors upon request.

CRediT authorship contribution statement

Manuel Contreras-Jara: methodology, formal analysis, visualization, writing (original draft preparation); Tomás Echaveguren: conceptualization, investigation, writing (review and editing); Eduardo Allen: methodology, formal analysis; Alondra Chamorro: conceptualization, writing (review and editing); José Vargas-Baecheler: conceptualization, methodology.

Competing Interests

The authors declare that they have no conflict of interest.

Acknowledgements

The authors thank Chile's National Research and Development Agency (ANID) for supporting the research presented in this article through the Research Center for Integrated Disaster Risk Management (CIGIDEN).





Financial Support

This work was supported by the Research Center for Integrated Disaster Risk Management (CIGIDEN), financed by the National Research and Development Agency (ANID) [Grant No. ANID/FONDAP/1523A0009].

References

550

- Alvarez-Garreton, C., Mendoza, P.A., Boisier, J. P., Addor, N., Galleguillos, M., Zambrano-Bigiarini, M., Lara, A., Puelma, C., Cortes, G., Garreaud, R., McPhee, J., and Ayala, A.: The CAMELS-CL dataset: catchment attributes and meteorology for large sample studies Chile dataset, Hydrol. Earth Syst. Sci., 22, 5817–5846, doi: 10.5194/hess-22-5817-2018, 2018.

 Arrighi, C., Brugioni, M., Castelli, F., Franceschini, S., and Mazzanti, B.: Flood risk assessment in art cities: the exemplary case of Florence (Italy), J. Flood Risk Manag., 11, 5616–5631, doi: 10.1111/jfr3.12226, 2018.
- Arseni, M., Rosu, A., Calmuc, M., Calmuc, V.A., Iticescu, C., and Georgescu, L.P.: Development of flood risk and hazard maps for the lower course of the Siret River, Romania, Sustainability, 12(16), 6588, doi: 10.3390/su12166588, 2020.

 Aven, T.: A risk concept applicable for both probabilistic and non-probabilistic perspectives, Saf. Sci., 49, 1080–1086, doi: 10.1016/j.ssci.2011.04.017, 2011.
- Bar-Gera, H.: Origin-Based Algorithm for the Traffic Assignment Problem, Transp. Sci., 36(4), 398–417, doi: 10.1287/trsc.36.4.398.549, 2002.
 - Beckmann, M., McGuire, C., and Winsten, C.: Studies in the economics of transportation (Working Paper RM-1488), RAND Corp., https://www.rand.org/pubs/research_memoranda/RM1488.html, 1955.
 - Berdica, K.: An introduction to road vulnerability: what has done is done and should be done, Transp. Policy, 9, 117–127, doi: 10.1016/S0967-070X(02)00011-2, 2002.
- Bocchini, P., and Frangopol, D.M.: Generalized bridge network performance analysis with correlation and time-variant reliability, Struct. Saf., 33(2), 155–164, doi: 10.1016/j.strusafe.2011.02.002, 2011.
 Chow, V.T., Maidment, D.R. and Mays, L. W.: Applied Hydrology. 1st Ed, McGraw-Hill Inc, ISBN 0-07-100174-3, 1988.
 Contreras-Jara, M., Echaveguren, T., Chamorro, A., and Vargas-Baecheler, J.: Estimation of exceedance probability of scour
 - on bridges using reliability principles, J. Hydrol. Eng., 26(8), 04021029, doi: 10.1061/(ASCE)HE.1943-5584.0002109, 2021.
- Contreras-Jara, M., Echaveguren, T., Vargas, J., Chamorro, A., and de Solminihac, H.: Reliability-Based Estimation of Traffic Interruption Probability due to Road Waterlogging, J. Adv. Transp., 2018, doi: 10.1155/2018/2850546, 2018.
 - de Moel, H., Jongman, B., Kreibich, H., Merz, B., Penning-Rowsell, E., and Ward, P.J.: Flood risk assessments at different spatial scales, Mitig. Adapt. Strateg. Glob. Change, 20, 865–890, http://doi.org/10.1007/s11027-015-9654-z, 2015.
 - Emanuelsson, M.A.E., McIntyre, N., Hunt, C.F., Mawle, R., Kitson, J., and Voulvoulis, N.: Flood risk assessment for infrastructure networks, J. Flood Risk Manag., 7, 31–41, doi: 10.1111/jfr3.12028, 2014.
 - Faturechi, R., and Miller-Hooks, E.: Measuring the Performance of Transportation Infrastructure Systems in Disasters: A Comprehensive Review, J. Infrastruct. Syst., 21(1), 04014025, doi: 10.1061/(ASCE)IS.1943-555X.0000212, 2014.





- Ford, A., Barr, S., Dawson, R. and James, P.: Transport Accessibility Analysis Using GIS: Assessing Sustainable Transport in London, ISPRS International Journal of Geo-Information, 4(1), 124 149. doi: 10.3390/ijgi4010124, 2015.
- Fuchs, S., Birkmann, J., and Glade, T.: Vulnerability assessment in natural hazard and risk analysis: current approaches and future challenges, Nat. Hazards, 64, 1969–1975, http://doi.org/10.1007/s11069-012-0352-9, 2012.
 - Gao, L., Liu, X., Wang, P., Deng, M., Zhu, Q., and Li, H.: Measuring road network topology vulnerability by Ricci curvature, Phys. A Stat. Mech. Appl., 527, 121071, doi: 10.1016/j.physa.2019.121071, 2019.
- Gouldby, B. and Samuels, P.: Language of Risk. Project Definition, HR Wallingford, Wallingford, United Kingdom, 560 FLOODsite File Report T32-04-01, 56 pp, 2005.
 - Hall, J., Dawson, R., Manning, L., Walkden, M., Dickson, M., and Sayers, P.: Managing changing risks to infrastructure systems, Proc. Inst. Civ. Eng. Civ. Eng., 159, 21–27, doi: 10.1680/cien.2006.159.6.21, 2006.
 - Herrera, E.K., Flannery, A., and Krimmer, M.: Risk and Resilience for Highway Assets, Transp. Res. Rec., 2604, 1–8, doi: 10.3141/2604-01, 2017.
- Hung, C.C., and Yau, W.G.: Vulnerability evaluation of scoured bridges under floods, Eng. Struct., 132, 288–299, doi: 10.1016/j.engstruct.2016.11.044, 2017.
 - Klinga, J.V., and Alipour, A.: Assessment of structural integrity of bridges under extreme scour conditions, Eng. Struct., 82, 55–71, doi: 10.1016/j.engstruct.2014.07.021, 2015.
 - Kron, W.: Flood Risk = Hazard Values Vulnerability, Water Int., 30(1), 58–68, doi: 10.1080/02508060508691837, 2005.
- Kumar, P.: Static Traffic Assignment using User Equilibrium and Stochastic User Equilibrium Python Code (V2.0), Zenodo [code], doi: 10.5281/zenodo.3479554, 2019.
 - Lam, J.C., and Adey, B.T.: Functional loss assessment and restoration analysis to quantify indirect consequences of hazards, ASCE-ASME J. Risk Uncertain. Eng. Syst. Part A: Civ. Eng., 2(4), 04016008, doi: 10.1061/AJRUA6.0000877, 2016.
- Lam, J.C., Heitzler, M., Adey, B.T., and Hurni, L.: Estimating network related risks: A methodology and an application in the transport sector, Nat. Hazards Earth Syst. Sci., 18(8), 2273–2293, doi: 10.5194/nhess-18-2273-2018, 2018a.
 - Ministry of Public Works (MOP): Diagnosis and classification of water streams and bodies of water according to quality objective: The Aconcagua river basin, General Directorate of Waters, Santiago, Chile, 160 pp., 2004.
 - Ministry of Public Works (MOP): Georeferenced observatory, MOP [data set], http://snia.dga.cl/observatorio, 2017.
- Ministry of Public Works (MOP): Hydrometeorological information and water quality online, MOP [data set], 580 http://snia.dga.cl/BNAConsultas/reportes, 2019a.
 - Ministry of Public Works (MOP): National Road Network 2020, MOP [data set], http://www.mapas.mop.cl/, 2020b.
 - Ministry of Public Works (MOP): National Traffic Survey 2019, MOP [data set],
 - http://sitministerial.maps.arcgis.com/apps/webappviewer/index.html?id=91ae27f8339a44f2bf0790da6ca47d36, 2020c.
- Ministry of Public Works (MOP): Road design guidelines of the Highways Manual, Highways Directorate, Santiago, Chile,
- 585 1544 pp., 2019b.



http://qgis.osgeo.org, 2021.



Ministry of Public Works (MOP): Update of HDM-4 Model Parameters, Contract DV N°2616 Final Report, Highways Directorate, Santiago, Chile, 124 pp., 2018.

- Ministry of Public Works (MOP): National Road Network Dimensions and Characteristics, Highways Directorate, Santiago, Chile, 304 pp., 2020a.
- Pyatkova, K., Chen, A., Djordjevic, S., Butler, D., Vojinovic, Z., Abebe, Y., Hammond, M.: Flood Impacts on Road Transportation Using Microscopic Traffic Modelling Techniques. In: Simulating Urban Traffic Scenarios; edited by: Behrisch, M. and Weber, M., Springer: Berlin, Heidelberg, Germany, 115–126, doi: 10.1007/978-3-319-33616-9, 2019.
 QGIS Development Team: QGIS Geographic Information System. Open Source Geospatial Foundation Project [software],
- 595 TRB (Eds.): Highway Capacity Manual. 3rd Edition, Transportation Research Board, Washington D.C., United States, ISBN-10 0309067464, 2000.
 - TRB (Eds): Highway Capacity Manual. A Guide for multimodal mobility analysis, 6th Edition, Transportation Research Board, Washington D.C., United States, ISBN 978-0-309-36997-8, 2016.
- U.S. Army Corps of Engineers (USACE): HEC-RAS River Analysis System User's Manual v5.0, Institute for Water Resources
 Hydrologic Engineering Center (CEIWR-HEC), California, United States, 960 pp., 2016.
 - Verni, F. and King, H.: Estimación de crecidas en cuencas no controladas, in: Proceedings of the 3rd National Colloquium of Hydraulic Engineering of the Chilean Society of Hydraulic Engineering, Santiago, Chile, 29 November 1 December, 357-374, 1977.

605